DOI: 10.13009/EUCASS2017-43

Smoke oxide particles formation at the burning surface of condensed systems

Valery A. Babuk, and Nikita L. Budnyi
Baltic state technical university «VOENMEH»
1, First Krasnoarmeyskaya Str., St.-Petersburg, 190005, Russia
E-mail: Babuk@peterlink.ru

Abstract

Main positions of the mathematical model of smoke oxide particles (SOPs) formation at the burning surface of condensed system are developed. The model includes description of SOPs formation during burning of non-agglomerating metal in gas phase near surface of the burning condensed system, and during burning of metal of agglomerating particles on the surface of skeleton layer. Results and perspectives of using the model are considered for two different condensed systems (based on active binder and based on ammonium nitrate), which produce SOPs mostly during realization of one of the mentioned mechanisms. A comparison of numerical and experimental results has allowed to make a conclusion about their satisfactory agreement. An analysis of the model allows to create a base for its future modernization and application.

1. Introduction

Aluminum is indispensable component of high-energy propellants (condensed systems). The specific feature of combustion of such systems is a formation of the condensed combustion products (CCPs), which is a result of high evaporation (dissociation) temperature of Al_2O_3. The CCPs properties have a significant effect on energetic system operation. They affect intensity of slag formation in the combustion chamber, characteristics of combustion products flow interaction with construction elements, optical properties of combustion products, operation stability.

It is generally accepted nowadays that the condensed products at the surface of burning propellant are formed and delivered in gas phase in two fractions: agglomerates and smoke oxide particles (SOPs) [1]. Agglomerates are product of coalescence of the condensed substances (aluminum and it oxide, as a rule) in a surface layer of condensed system. Their size can reach hundreds and even thousand micrometers. Smoke oxide particles are formed as a result of metal combustion in vicinity of the burning propellant surface in gas phase. The size of these particles, as a rule, does not exceed several micrometers.

The present work is devoted to mathematical modeling of SOPs formation at the surface of burning condensed systems. There are no works known for us that covers this problem.

Smoke oxide particles are formed as a result of realization of two mechanisms [2]. The first mechanism is SOPs formation as a result of combustion of non-agglomerating metal in vicinity of condensed system burning surface; the second mechanism – SOPs formation during burning of agglomerating particles at the surface of skeleton layer. The description of SOPs formation during realization of specified above mechanisms is presented below.

2. Smoke oxide particles formation during burning of non-agglomerating metal

Non-agglomerating metal occurs because some fraction of metal fuel does not take part in a formation of skeleton layer (SL) and in an agglomeration process as a rule [3]. Skeleton layer doesn't occur only at the specific conditions determined by propellant composition. These conditions are determined by the possibility of carbon skeleton formation during binder decomposition. Presence of the carbon skeleton is an indispensable condition for SL formation. In the case of absence of SL, the burning surface of propellant can be considered as a classical burning surface, i.e. an interface of two phases: condensed and gas.. The example of situation when SL is absent and almost whole totality of metal fuel does not agglomerate is a combustion of active binder based propellants at high pressure [4]. It can be assumed that almost all SOPs particles at the surface are product of non-agglomerating metal combustion. Further analysis is focused mainly on process description applied to combustion of the active binder-based propellant under high pressure.

2.1 Gas phase properties

DOI: 10.13009/EUCASS2017-43

Active binder can be considered as a monopropellant. Simplified estimation of gas phase properties can be given using Belyaev-Zel'dovich model [5]. The flame front height above the burning surface can be calculated using Belyaev-Zel'dovich model in following way:

$$l_b = \frac{\lambda_{gas}}{\rho_{gas} u_{gas} c_{gas}} \ln \frac{T_b - T^*}{T_s - T^*}, \quad (1)$$

where: T_b – combustion products temperature, T_s – burning surface temperature, ρ_{gas}, u_{gas}, c_{gas}, λ_{gas} – density, velocity, specific heat capacity and heat conductivity of gas phase respectively, T^* is:

$$T^* = T_s + \frac{Q_s - c_{prop}(T_s - T_0)}{c_{gas}}, \quad (2)$$

where: T_0 – initial temperature of the propellant, Q_s – heat of reaction, c_{prop} – specific heat capacity of condensed matter. The temperature profile in gas phase can be calculated using following formula:

$$T(x) = T^* + (T_s - T^*) \exp \frac{\rho_{gas} u_{gas} c_{gas}}{\lambda_{gas}} x, \quad (3)$$

where x – spatial coordinate directed from burning surface to gas. Gas composition above the reaction front is considered as equilibrium. Gas composition and temperature is calculated using equilibrium thermodynamics [6].

2.2 The physical picture of ignition and heterogeneous burning of metal particles

The analysis of literature references has allowed to formulate following physical picture of metal particles behavior during combustion of condensed system.

A protective oxide film covers initial particles. It is assumed that oxide film is crystalline. The results of different researches ([7] and others) show that oxide film can be in different phases (crystalline or amorphous), and it depends on manufacturing technology of the metal particles, temperature and duration of the process etc. During passing of the combustion wave, the particle is being exposed to the high-speed heating and it is leading to oxide film rupture. The rupture degree depends on thermomechanical loading rate, which is determined by the propellant burning rate and its thermophysical properties. Fast reaction of «pure» metal with oxidizer gas starts after the oxide film rupture. It is assumed that the linear oxidation law describes kinetics of this process. "Healing" of cracks in oxide film occurs after increasing of oxide film thickness over cracked places and then reaction continues according to the parabolic oxidation law. It is known that increase of oxide film thickness above some "critical" value (20-30 Å according to [8]) causes drop of the oxidation rate. Further, the secondary film rupture and "healing" are possible to occur. After temperature increase above ≈2303 K, the melting of oxide film occurs and it results in the drop of diffusion resistance of the film. The ignition moment corresponds to the heat explosion conditions.

After temperature increase above boiling temperature of the particle materials, the high-speed fragmentation of particles can occur. The secondary oxide droplets form final combustion products, the secondary metal droplets burn in heterogeneous or vapor-phase mode and form condensed combustion products. According to [1], pressure increase and particle size decrease result in higher probability of fragmentation.

In the issue, the process stages can be summarized as follows:

- Particle heating and possible oxide film rupture;
- Metal core melting and possible oxide film rupture;
- Heterogeneous oxidation (before oxide film melting);
- Oxide film melting;
- Heterogeneous oxidation through liquid oxide film;
- Particle boiling and possible fragmentation.

DOI: 10.13009/EUCASS2017-43

2.3 Mechanical state of particle

The behavior of a particle in the burning process significantly depends on mechanical integrity the protective oxide film. Its rupture is possible due to thermal stresses and distinction of the specific volume of reacting aluminum and forming oxide (Pilling-Bedworth ratio for Al_2O_3 is greater than 1). The results of [9-11] are taken as a base for our mathematical description. It is based on the linear elasticity theory. The fracture criterion is equivalent stress exceeding over critical stress at the metal-oxide interface:

$$\sigma_{eq} \geq \sigma_{cr} \tag{4}$$

The critical stress is calculated using Griffith fracture theory. Figure 1 shows some example of the model parametrical study results.

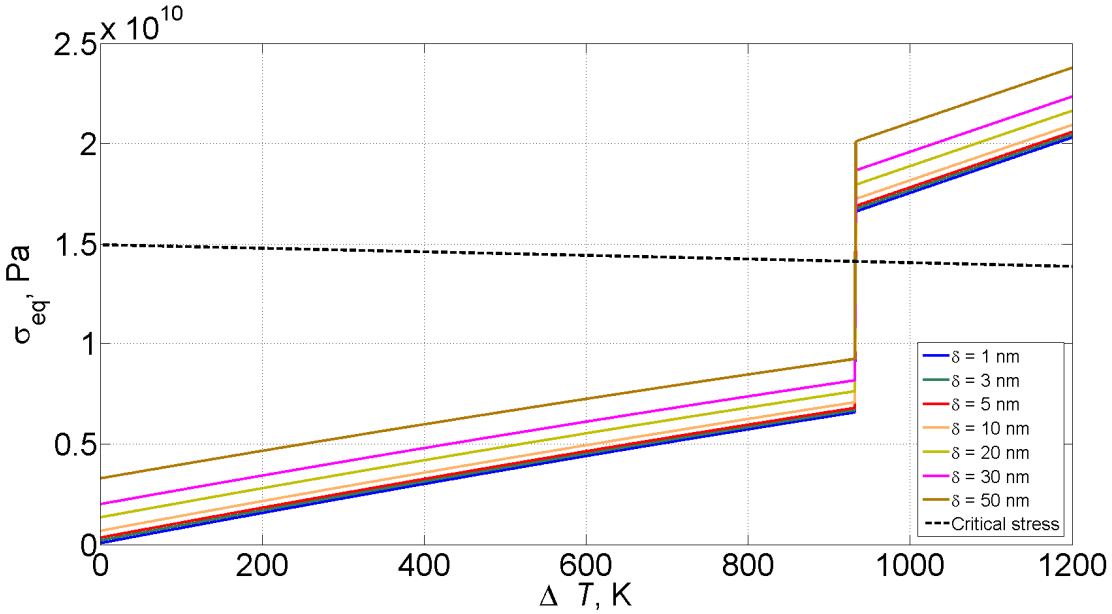

Figure 1: Example of dependence of equivalent stress vs overheat for different thickness of the oxide film (δ)

Parametrical study results allow to make some conclusions:
- There is abrupt stress increase when metal core melts, that probably leads to the oxide film rupture;
- In the case of thin oxide film, its rupture is more likely caused by the metal core melting;
- Increase of oxide film thickness leads to stress increases due to effect of distinction of the specific volume of reacting aluminum and its forming oxide;
- Oxide film rupture before the metal core melting is possible only in the case of quite thick film (greater than 30 nm);
- Particles radius decrease leads to stress increase if oxide film thickness remains constant. As a result, a lower overheat causes rupture.

The condition (4) tells only about the rupture fact. Fraction of metal core surface which is free from oxide cover (χ) is also important for the ignition process. It is assumed, that this parameter can be estimated as:

$$\chi = k \cdot \frac{dT}{dt}_{\sigma_{eq}=\sigma_{cr}} \tag{5}$$

where: k – matching coefficient, which value determines during matching of numerical and experimental data.

The linear form of (5) is just a first estimation. Further, the form of $\chi(dT/dt)$ has to be modified possibly. Let us note that the influence of thermomechanical loading rate on the oxide film rupture degree and, as a result, on ignition temperature in condensed systems was noted in several works early [7].

DOI: 10.13009/EUCASS2017-43

2.4 Oxidation and heterogeneous burning of metal particle

A mathematical description of process is based on equations of mass, energy and momentum conservation, and on the description of mechanical state (mentioned above). It is assumed that the main effect on ignition dynamics is given by oxidation at places where oxide cracks occur. The “classical” oxidation laws [7] describe oxidation kinetics. The used forms of equations are similar to [12].

Let us mention some details. It is assumed that in the case of the secondary film rupture, the cracks occurs in the same places where they were during the primary rupture, and the fraction of metal core surface free of oxide remains the same.

Particle motion describes as follows:

$$\begin{cases} \dfrac{du_p}{dt} = \dfrac{C_D \Omega_{mid} \rho_{gas} \left| u_{gas} - u_p \right| \left(u_{gas} - u_p \right)}{2(m_{Al} + m_{Al2O3})} \\ \dfrac{dx}{dt} = u_p \end{cases} \tag{6}$$

where: x – spatial coordinate, C_D – drag coefficient, Ω_{mid} – midsection area, m_{Al}, m_{Al2O3} – metal and oxide mass, u_{gas}, u_p – velocity of gas and particle, ρ_{gas} – gas density.

Gas phase properties are calculated according to 1.1. Figure 2 shows the example of temperature calculation as a function of spatial coordinate - x. One can note oxide film rupture and “healing”, combustion stages and modes changes. In this case, we have to talk about “forced” ignition, because the kinetic flame temperature quickly becomes greater than a particle ignition temperature.

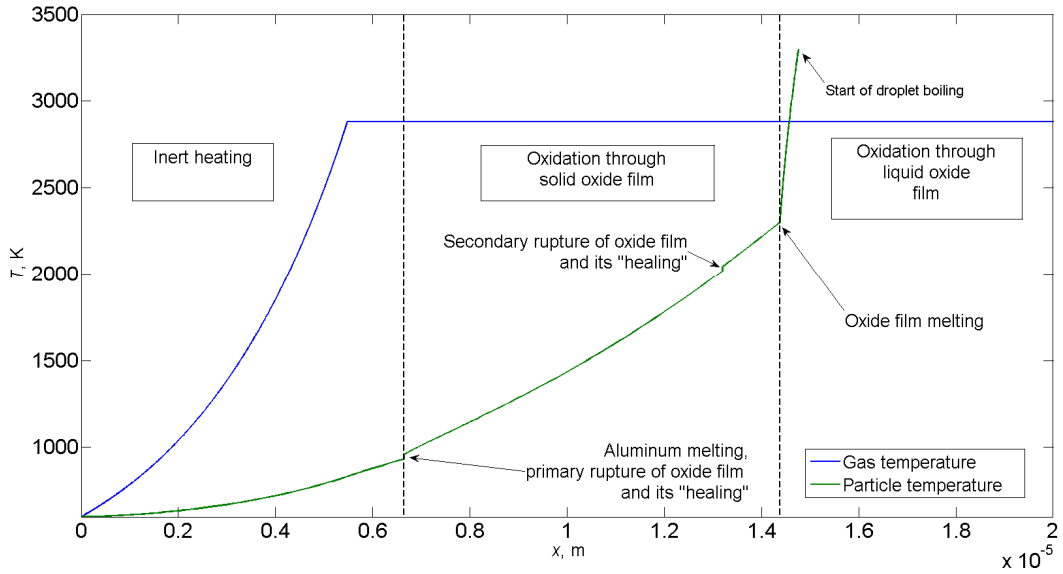

Figure 2: Calculation example for a single particle

2.5 Particle boiling

Particle boiling process and further fragmentation are quite complex phenomena. Let us accept following physical picture.

DOI: 10.13009/EUCASS2017-43

Chemical interaction between condensed metal and its oxide (Al^c +$Al_2O_3{}^c$) with gas products formation is more probable than metal evaporation in thermodynamic meaning [13]. However, realization of this process is possible only if suitable nucleation centers exist. Let us assume that their size does not exceed the size of the adsorption layer. In this case, the overheat degree can be significant. Gas bubbles in the size ~ 100 nanometers are formed at interaction Al^c +$Al_2O_3{}^c$. These sizes are sufficient for irreversible process of metal evaporation. Gas gap is formed between metal and oxide, and its growth can lead to a fragmentation of oxide and metal core (figure 3).

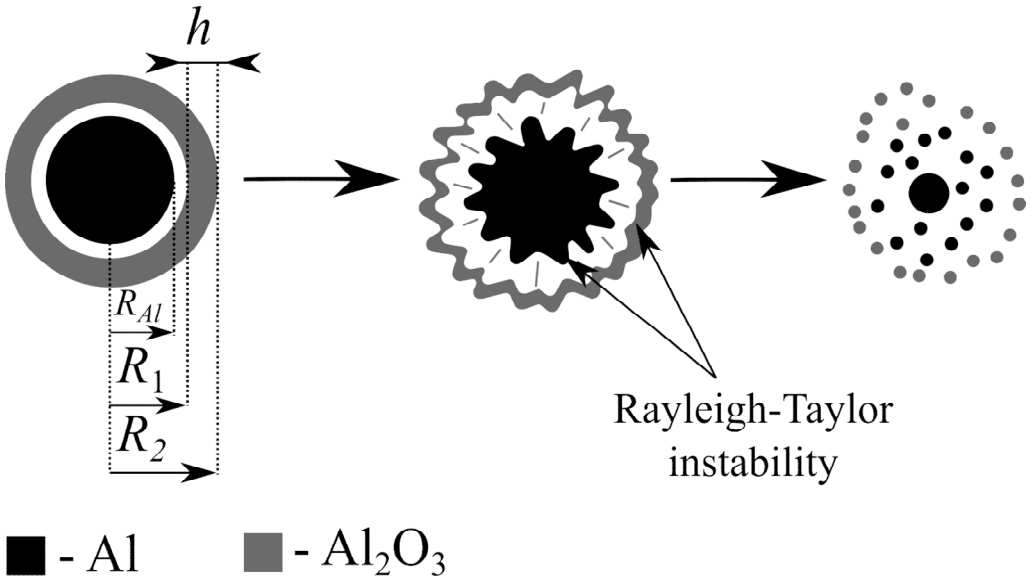

Figure 3: Scheme of particle after the beginning of evaporation.

Character of process depends on its dynamics. The description is based on mass and energy conservation equations:

$$Q = \frac{dT}{dt}\left\{c_{vox}M_{ox} + c_{vm}M_m + c_{v_g}M_g\right\} + (c_{v_g} - c_{vm})TG_g + P\frac{dV_g}{dt} + \frac{dE_{kin}}{dt} + \sigma\frac{d}{dt}\left(\Omega_1 + \Omega_2\right) \quad (7)$$

$$\frac{dM_g}{dt} = -\frac{dM_m}{dt} = G_g \quad (8)$$

These equations are complemented by the equation of ideal gas state and the equations of liquid shell expansion dynamics, which are based on mass and momentum conservation equations for liquid film:

$$PV_g = \frac{M_g}{\mu_g}R_0T \quad (9)$$

$$(R_1\ddot{R}_1 + 2\dot{R}_1^2)\left[1 - \frac{R_1}{R_2}(1 - \frac{\rho_{out}}{\rho_{ox}})\right] + \frac{1}{2}\dot{R}_1^2\left[\frac{R_1^4}{R_2^4}(1 - \frac{\rho_{out}}{\rho_{ox}}) - 1\right] = \frac{1}{\rho_{ox}}\left[P - P_{out} - \frac{2\sigma}{R_1} - \frac{2\sigma}{R_2}\right]$$

$$\dot{R}_2 = \dot{R}_1\frac{R_1^2}{R_2^2} \quad (10)$$

where: T – particle temperature, c_{vm}, c_{vox}, c_{vg} – specific isochoric heat capacity of metal, oxide and evaporation products respectively, M_m, M_{ox}, M_g – mass of metal particle, oxide film and evaporation products, Q – net heat flux, E_{kin} – liquid shell kinetic energy ($E_{kin} \approx M_{ox}\dot{R}_1^2/2$), V_g – evaporation products volume, P – pressure of evaporation products, P_{out} – ambient pressure, σ - surface tension between oxide and gas, Ω_1, Ω_2 – inner and outer surfaces of liquid shell respectively, ρ_{ox}, ρ_{out} – oxide and ambient gas density respectively, G_g – mass flux of evaporating metal, calculated as follows

DOI: 10.13009/EUCASS2017-43

$$G_g = \mu_g \omega_v \Omega_m \tag{11}$$

where μ_g – metal molar mass, Ω_m – metal core surface, and specific molar flux of evaporating metal can be calculated as follows:

$$\omega_v = A_1 \exp\left(-\frac{E_a}{R_0 T}\right)\frac{1}{\sqrt{T}}(P_S - P) \tag{12}$$

where P_s – saturated pressure at temperature T, A_1 – pre-exponential factor, E_a – activation energy.

System (7)-(8) with (9)-(10) integrates for some initial conditions. There are some assumptions: oxide mass remain the same, vapor transport through oxide film is absent, the state of surface layer between a gas phase and liquid oxide film is equilibrium.

Integration allows to obtain temperature, evaporation products pressure, and geometrical parameters (R_1, R_2, h) as functions of time. During gaseous cavity growth and liquid shell expansion, the conditions for development of Rayleigh-Taylor instability occur (fig. 3). Physical picture and mathematical description of spherical liquid shells expansion and fragmentation are presented in [14]. According to this work, piercing of “holes” in liquid shell occurs during instability development. Then these “holes” contract into “rims” which collide into “ligaments”. Breakup of the “ligaments" is a “source” of secondary droplets distribution. It is assumed that in the moment of the breakup of liquid shell value of disturbance on “most dangerous” wavelength becomes comparable with liquid shell thickness – this is a formalization of the breakup condition.

The mathematical description from [14] provides a fragmentation criterion, which depends on shell acceleration, density, surface tension etc. Mean droplet diameter can be calculated as follows [14]:

$$\langle d \rangle \approx 1.5\sqrt{\lambda^* h^*} \tag{13}$$

where: λ^*, h^* – «most dangerous» wavelength and shell thickness at the moment of break-up.

Distribution of secondary droplets is described as follows [14]:

$$f(x = d/\langle d \rangle) = \frac{n^n}{\Gamma(n)} x^{n-1} e^{-nx} \tag{14}$$

where $n \approx 4$; $\Gamma(n)$ – gamma-function.

High acceleration of gas-liquid interface can cause disturbance growth at the metal core surface and its fragmentation too. Mean diameter of the metal secondary droplets can be roughly estimated in following way [15]:

$$\lambda_{Al}^* = (2/3)^{1/2}\pi(\ddot{R}_1^* \rho_m / \sigma_m)^{-1/2} \approx \langle d_{Al} \rangle \tag{15}$$

where: ρ_m, σ_m – density and surface tension of metal respectively.

In the case of low accelerations of liquid shell, the process probably becomes unsymmetrical [14]. This phenomenon appears in non-simultaneous “holes” formation. Furthermore, in the case of low acceleration, the “most dangerous” wavelength becomes larger. By our mind, in the case of low loading rate, the catastrophic fragmentation is less probable and “smooth” transformation of liquid film into oxide droplet (oxide “cap”) is more probable.

Primary parametric study shows that the catastrophic fragmentation is more probable in cases of high pressure and smaller particle sizes. These conclusions correspond to experimental data on agglomerates [1, 26]

DOI: 10.13009/EUCASS2017-43

2.6 Combustion of metal particles after liquid film breakup

After liquid film breakup, several scenarios of combustion can occur. If particle integrity remains and it has relatively large size (or if particle undergoes fragmentation, bur secondary metal droplets are relatively large), then burning continues in vapor-phase mode. Oxide formation takes place in gas phase. Ions act as nuclei, most likely [16]. Diameter of the forming oxide particles is 100-300 nm. If fine fragmentation of metal core occurs, then secondary droplets combust in a heterogeneous mode. This behavior caused by several factors: intensification of heat and mass transfer [17-20], changing of flow regime from continuous to transition and free-molecular [21]. Some "moderate" sized particles burn in diffusion-kinetic mode, when oxide is forming in gas phase and on the particle surface. During decreasing of burning particles size, chemical reaction moves to the surfaces. Therefore, oxide particles sizes depends on fragmentation process (its presence or absence, and its fineness) significantly.
Figure 4 shows oxide formation after liquid oxide film breakup.

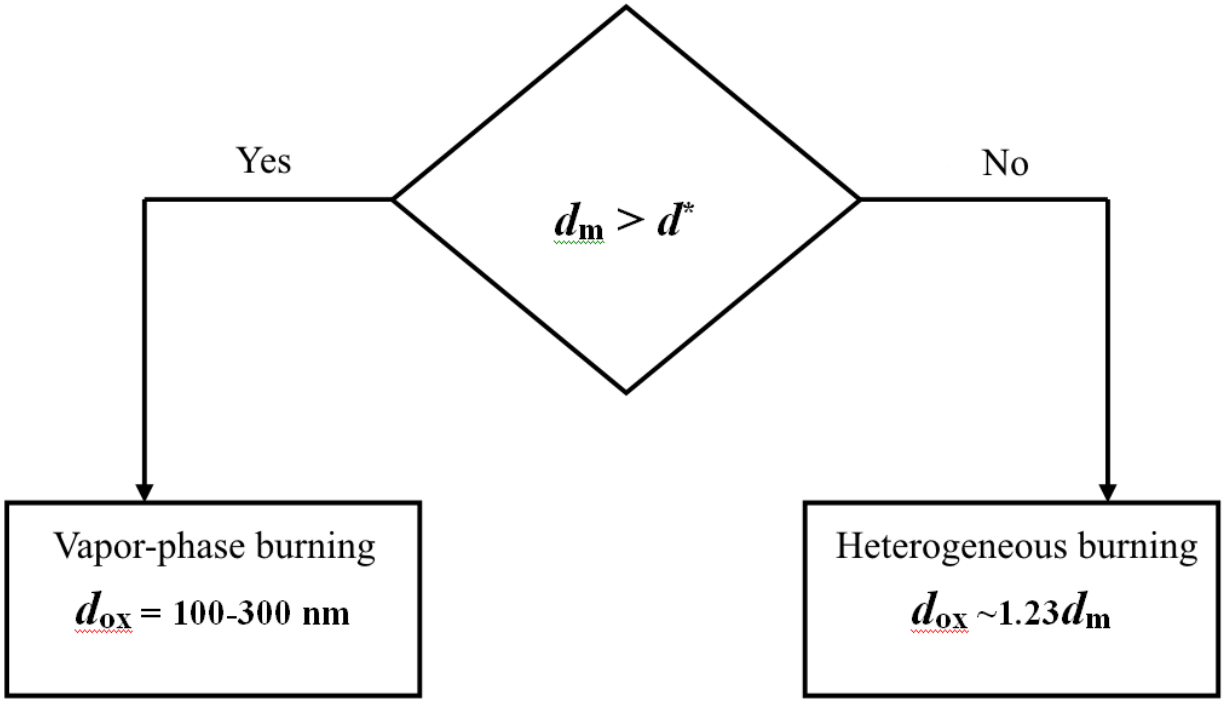

Figure 4: Scheme of SOPs formation (d_m – secondary metal droplet diameter after fragmentation, d_{ox} – oxide particle diameter, d^* - particle diameter corresponding to condition of equality of diffusion mass flux and mass reaction rate).

2.7 Analysis of the model

The developed description can be used for estimation of sizes of SOPs formed during combustion of condensed systems based on active binder at high pressure [22].

Estimation shows that ~25-30% mass of metal particle combusts in heterogeneous mode before metal boiling. Sizes of the secondary oxide droplets that formed during fragmentation are calculated using formulas (13)-(14). The secondary metal droplets combust in heterogeneous and vapor-phase mode (figure 4).

The developed description allows to give an interpretation of experimental data on SOPs sizes during combustion of propellants based on active binder (figure 5, [4]). Bimodal distribution is a result of realization of two mechanism of SOPs formation. Relatively small mass of the first mode allows to assume that d^* is relatively large. Mass and sizes of second fraction allows to assume that intensity of fragmentation during combustion is high. Let us make an assumption that fragmentation intensity and its fineness is the one of the causes of distinction in sizes of SOPs second fraction that formed during combustion of non-agglomerating metal in condensed systems and during combustion of aluminum dust-air mixtures [27]. There is an assumption that probability of fragmentation during particles combustion in aluminum dust-air mixtures at low pressure is relatively low.

DOI: 10.13009/EUCASS2017-43

Summarize, developed description explains the nature of SOPs formation: main mechanism of SOPs formation is a heterogeneous combustion of metal particles.

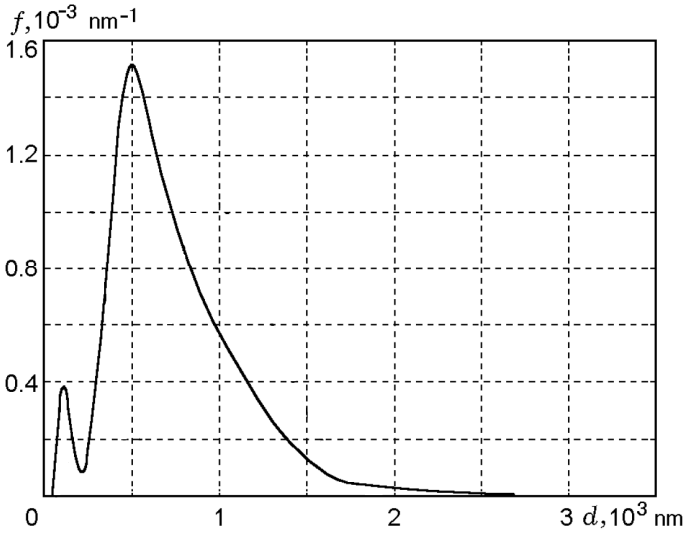

Figure 5: Mass function of size distribution density of smoke oxide particles for active binder-base propellant (P = 6 MPa).

3. Smoke oxide particles formation during burning of agglomerating metal

Agglomerating particles at the upper part of SL are involved in evolution process [23]. One of processes of evolution is a vapor-phase burning with SOPs formation. Model of the SOPs formation during vapor-phase burning of agglomerate metal was used to describe this phenomenon [24]. The model is consist of the system of ordinary differential equation described mass and concentration changes of SOPs fractions during their motion in a vicinity of burning agglomerate and enlargement caused by sub-oxide vapors condensation on their surfaces.

3.1 Informational support of the model

Let us consider the information support of the model:
- Soot particles act as condensation nuclei. Experimental data about the content and the size of soot particles in combustion products of solid propellants are very limited. There are no mathematical models describing soot formation. The data from [25] was used: size distribution of soot particles shown on figure 6.
- Properties of agglomerates (size, chemical content, structure) can be defined using experimental data [22] or mathematical modeling [26].
- Ambient gas properties (temperature, partial pressure of oxidizing components) can be calculated using methods from [23, 26].
- Residence time of agglomerate on the upper part of SL determines share of combusted metal and, consequently, SOPs mass. The residence time can be calculated using methods from [26].
- Parameters of gas flow around particle can be determined using data on burning rate of condensed system, its formulation, and operational pressure.

DOI: 10.13009/EUCASS2017-43

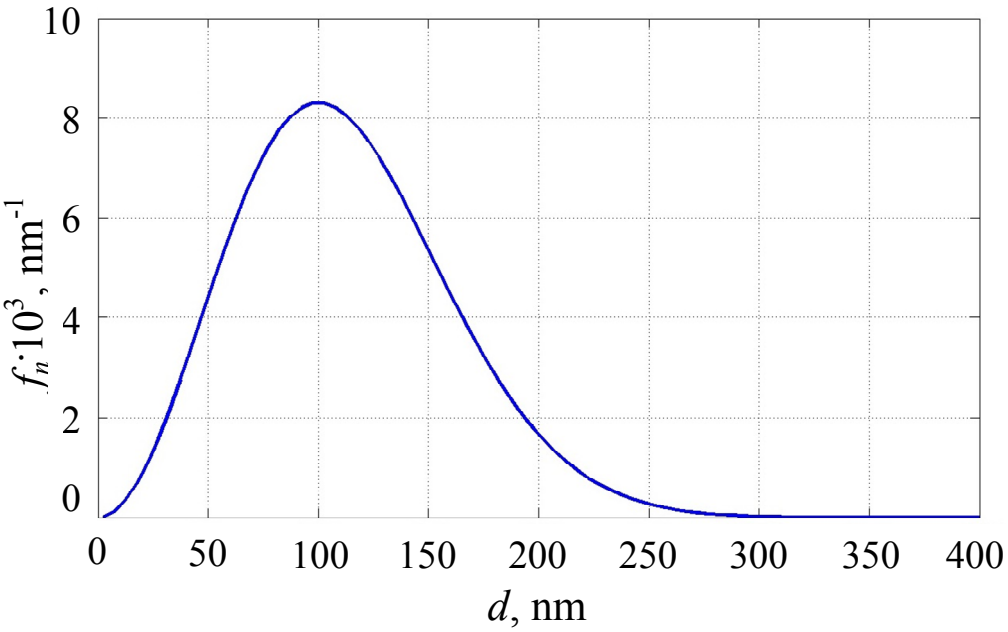

Figure 6: Function of size distribution density of soot particles

3.2 Testing the model

Data obtained for propellants on the basis of ammonium nitrate has been used for model testing. Those propellants have a specific feature: almost whole mass of metal fuel is involved in agglomeration [22]. Therefore, characteristics of SOPs are determined by agglomerates vapor-phase burning during their evolution at the surface. Figure 7 shows experimental mass distribution density function of agglomerates.

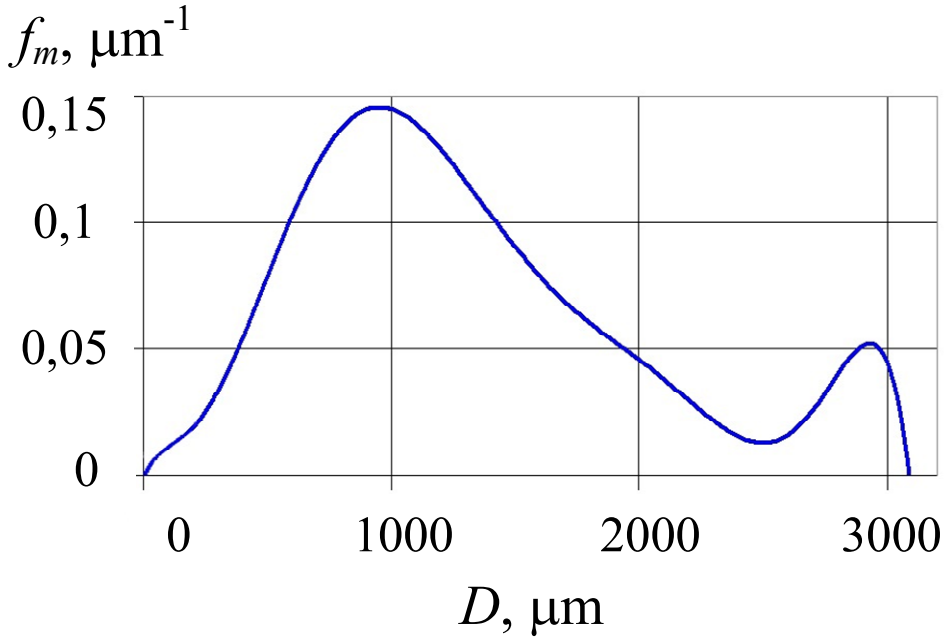

Figure 7: Mass function of size distribution density of agglomerates (P = 6 MPa)

DOI: 10.13009/EUCASS2017-43

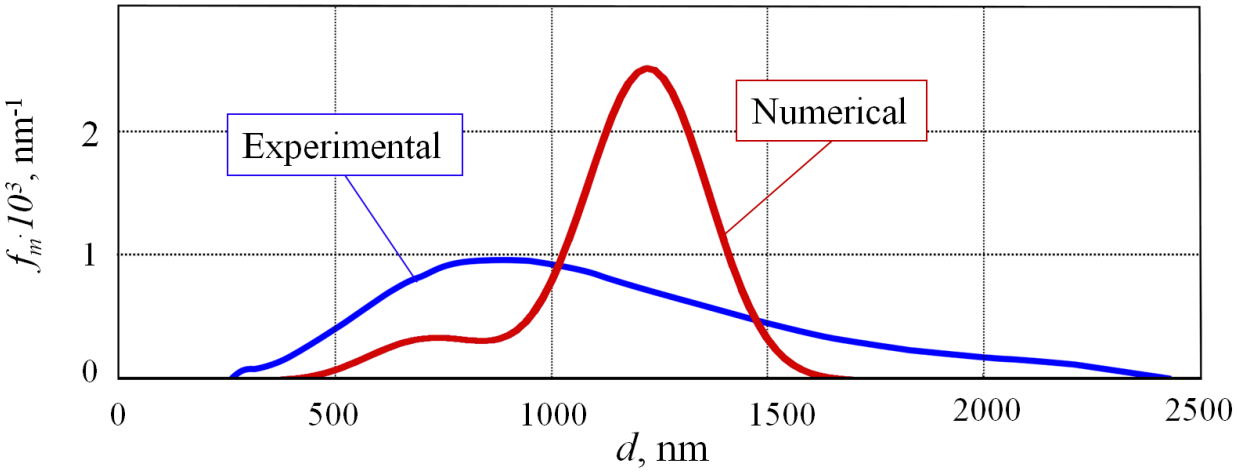

Figure 8: Mass function of size distribution density of smoke oxide particles for studied formulation (P = 6 MPa)

The comparison of numerical and experimental results are shown of figure 8. They allow to make a conclusion about qualitative and quantitative agreement. Numerical mass-mean diameter (1.16 μm) is close to experimental one (1.11 μm). One can say about distinction in other moments of distribution. There are some reasons to think that these distinctions are caused by uncertainty of the data on soot content and dispersity.

Conclusion

The developed mathematical model describes SOPs formation at the burning surface of solid propellants. It includes the model of SOPs formation during combustion of non-agglomerating metal and the model of SOPs formation during burning of agglomerating particles at the upper part of SL. Comparison of experimental and numerical data allows to make a conclusion about their agreement. The obtained results open possibilities for forecasting of SOPs dispersity at burning of any propellants under condition of the description of agglomeration process.

References

[1] Babuk, V.A., Vasilyev, V.A., and Malakhov, M.S. 1999. Condensed Combustion Products at the Burning Surface of Aluminized Solid Propellant. *Journal of Propulsion and Power*. 15(6): 783-793.

[2] Babuk, V. A. 2007. Problems in Studying Formation of Smoke Oxide Particles in Combustion of Aluminized Solid Propellants. *Combustion, Explosion, and Shock Waves*. 43(1): 38-45.

[3] Babuk, V. A. 2009. Properties of the Surface Layer and Combustion Behavior of Metalized Solid Propellants. *Combustion, Explosion, and Shock Waves*. 45(4): 486–494.

[4] Babuk, V. A, Dolotkazin, I. N, Glebov, A. A. 2005. Burning Mechanism of Aluminized Solid Rocket Propellants Based on Energetic Binders. *Propellants, Explosives and Pyrotechnics*. 30(4): 281-290.

[5] Novozhilov, B. V. 1973. Unsteady combustion of solid propellants. Moscow, Nauka (In Russian).

[6] Thermodynamic and thermophysical properties of combustion products. 1971. Ed.: Glushko, V. P. Moscow. VINITI Publishing (In Russian).

[7] Pokhil, P.F., Belyaev, A.F., Frolov, Yu.V., Logachev, V.S., Korotkov, A.I. 1972. Combustion of powdered metals in active media. Moscow. Nauka (in Russian).

[8] Maurakh, M. A., Mitin, B. S. 1979. Liquid refractory oxides. Moscow. Metallurgiya (In Russian).

[9] Rosenband, V. I., Vaganova, N. I. 1992. A strength model of heterogeneous ignition of metal particles. *Combustion, Explosion and Shock Waves*. 28(1): 1-7.

[10] Rosenband, V., Gany, A., Timnat, Y.M. 1995. Effect of mechanical stresses on heterogeneous oxidation of metals. *Oxidation of Metals*, 43:141–156.

[11] Rosenband, V. and Gany, A. 2001. Microscopic and Analytic Study of Aluminum Particles Agglomeration. *Combustion Science and Technology*. 166(1): 91-108.

[12] Babuk, V. A., Dolotkazin, I., Gamsov, A., Glebov, A., DeLuca, L. T., Galfetti, L. 2009. Nanoaluminum as a Solid Propellant Fuel. *Journal of Propulsion and Power*. 25(2): 482-489.

[13] Babuk, V. A., Vasilyev, V. A. 2002. Model of Aluminum Agglomerate Evolution in Combustion Products of Solid Rocket Propellant. *Journal of Propulsion and Power*. 18: 814-824.

DOI: 10.13009/EUCASS2017-43

[14] Vledouts, A., Quinard, J., Vandenberghe, N., Villermaux, E. 2016. Explosive fragmentation of liquid shells. *J. Fluid Mech*.788: 246-273.
[15] Inoue, A., Aritomi, M., Takahashi, M., Tomita, Yo. 1992. An Analitical Model on Vapor Explosion of a High Temperature Molten Metal Drop in Water Induced by a Pressure Pulse. *Chemical Engineering Communications*, 118(1): 189-206.
[16] Zolotko, A. N., Vovchuk, Ya. I., Poletayev, N. I., Florko, A. V., Al'tman, I. S. 1996. Synthesis of nanooxides in two-phase laminar flames. *Combustion, Explosion and Shock Waves.* 32(3): 262-269.
[17] Bazyn, T., Krier, H., Glumac, N. 2007. Evidence for the transition from diffusion-limit in aluminum particle combustion // Proceedings of the Combustion Institute 31, pp. 2021-2028.
[18] P. Bucher, R. A. Yetter, F. L. Dryer. 1996. Flame structure measurement of single, isolated aluminum particles burning in air. *Twenty-Sixth Symposium (International) on Combustion/The Combustion Institute*, 1899–1908.
[19] Sundaram, D. S., Puri, P., Yang, V. 2016. A general theory of ignition and combustion of nano-and micron-sized aluminum particles. *Combustion and Flame*, 169: 94-109.
[20] Sundaram, D. S., Yang, V., Zarko, V. E. 2015. Combustion of nano aluminum particles (Review)**.** *Combustion, Explosion and Shock Waves*. 51(2): 173-196.
[21] Mohan, S., Trunov, M. A., Dreizin, E. L. 2009. On Possibility of vapor-phase combustion for fine aluminum particles. *Combustion and Flame*. 156: 2213-2216.
[22] Babuk, V. A. Formulation Factors and Properties of Condensed Combustion Products. *In "Chemical Rocket Propulsion. A Comprehensive Survey of Energetic Materials"*, pp. 319-341, Springer, 2017, Chapter 13.
[23] Babuk, V. A., Ildar N. Dolotkazin, I. N., Nizyaev, A. A. Analysis and Synthesis of Solutions for the Agglomeration Process Modeling / *EUCASS Book Series Advances in Aerospace Sciences Vol. 4 – Progress in Propulsion Physics,* EUCASS, Torus Press, EDP Sciences, Paris, 2013, pp. 33-58.
[24] Babuk, V. A., Budnyi, N. L., Nizyaev A. A. Mathematical modeling of agglomerates evolution. Proceedings of 6th European Conference for Aerospace Sciences, Krakow, 28th June - 3rd July 2015, Poland.
[25] Arkhipov, V. A., Ratanov, G. S. 1979. Laser diagnostics methods for solid combustion products. *Combustion, Explosion and Shock Waves*.15(2):282-284.
[26] Babuk, V. A., Ivonenko, A. N., Nizyaev, A. A. 2015. Calculation of the characteristics of agglomerates during combustion of high-energy composite solid propellants. *Combustion, Explosion and Shock Waves*. 51(5): 549-559.
[27] Yagodnikov, D. A., Gusachenko, E. I. 2002. Effect of an external electric field on the disperse composition of condensed products of aluminum particle combustion in air. *Combustion, Explosion and Shock Waves*. 38(4): 449-455.